Title	Surface plasmon resonance in gold nanoparticle infiltrated dielectric opals
Authors	Romanov, Sergei G.;Susha, A. S.;Torres, C. M. Sotomayor;Liang, Z.;Caruso, F.
Publication date	2005-04-04
Original Citation	Romanov, S. G., Susha, A. S., Torres, C. M. S., Liang, Z. and Caruso, F. (2005) 'Surface plasmon resonance in gold nanoparticle infiltrated dielectric opals', Journal of Applied Physics, 97(8), pp. 086103. doi: 10.1063/1.1875735
Type of publication	Article (peer-reviewed)
Link to publisher's version	http://aip.scitation.org/doi/abs/10.1063/1.1875735 - 10.1063/1.1875735
Rights	© 2005 American Institute of Physics, This article may be downloaded for personal use only. Any other use requires prior permission of the author and AIP Publishing. The following article appeared in Romanov, S. G., Susha, A. S., Torres, C. M. S., Liang, Z. and Caruso, F. (2005) 'Surface plasmon resonance in gold nanoparticle infiltrated dielectric opals', Journal of Applied Physics, 97(8), pp. 086103 and may be found at http://aip.scitation.org/doi/abs/10.1063/1.1875735
Download date	2024-04-24 23:42:15
Item downloaded from	https://hdl.handle.net/10468/4232

Surface plasmon resonance in gold nanoparticle infiltrated dielectric opals

S. G. RomanovA. S. SushaC. M. Sotomayor TorresZ. Liang and F. Caruso

Surface plasmon resonance in gold nanoparticle infiltrated dielectric opals

S. G. Romanov[a),b)]
University of Wuppertal, Institute of Materials Science, Department of Electrical Information and Media Engineering, Gauss Str. 20, 42097, Wuppertal, Germany

A. S. Susha
Photonics and Optoelectronics Group, Department of Physics and CeNS, University of Munich, 80799 Munich, Germany

C. M. Sotomayor Torres
NMRC, University College Cork, Lee Maltings, Prospect Row, Cork, Ireland

Z. Liang and F. Caruso
Department of Chemical and Biomolecular Engineering, University of Melbourne, Victoria 3010, Australia

Light reflectance in three-dimensional metallo-dielectric photonic crystals of polyelectrolyte-coated latex spheres infiltrated with gold nanoparticles has been studied. Broad directional reflectance bands associated with the surface plasmon resonance in the lattice of the gold nanoparticle shells are observed in a wavelength range well separated from the diffraction resonance of the opal lattice. Dependence of surface plasmon resonance spectra on the Au nanoparticle distribution has been demonstrated. © *2005 American Institute of Physics.* [DOI: 10.1063/1.1875735]

Substituting dielectrics with metals in photonic crystals (PhCs) is a way towards robust omnidirectional photonic band gap materials.[1,2] However, technological challenges associated with the synthesis of submicrometer-sized metal spheres and their assembly in a crystal have not been yet resolved. Mimicking metal spheres, metallo-dielectric core-shell spheres with a gold coating synthesized on silica beads were recently realized and assembled in a regular lattice.[3,4] Alternatively, gold nanoshells were formed depositing gold colloid nanoparticles (NPs) on polymer spheres.[5] Opal-like assemblies of Au nanoshells exhibit a superposition of the lattice diffraction resonance and the surface plasmon resonance (SPR).[6] Despite the wide spectral separation of these resonances, the dispersion of the Au NP opal diffraction resonance is squeezed due to the strong frequency dependence of the dielectric constant of the composite introduced by the Au NPs. In fact, the SPR in opals assembled from Au nanoshells is split into several bands, the central frequencies of which are, generally, independent on the lattice rotation while the band intensities are directionally dependent.[6,7] The isotropy of SPR can be a consequence of the spherical symmetry of core-shell beads, whereas the SPR band magnitude becomes a function of the nanoshell interaction.

One method, which avoids difficulties in packing heavy metal beads, is the infiltration of pre-assembled opals with metal NPs. To facilitate homogeneity of the NP distribution in the opals, polyelectrolyte (PE) multilayer-coated spheres were used to form the opals.[5] The PE layers act as a matrix for uptake and immobilization of the metal NPs on the sphere surface. In this article, we compare the visible and near infrared (NIR) optical reflectance spectra of Au nanoshell opals and Au-infiltrated opals.

Opal films of 10–12 μm thickness were crystallized from core-shell polystyrene (PS) beads of 640-nm-diam (D) coated by two, four, six, and eight electrically charged PE layers. Since the outermost PE layer is oppositely charged with respect to the positively charged 4-dimethylaminopyridine-stabilized 6-nm-diameter Au NPs, the electrostatic forces lead to binding and dense impregnation of the PE template with Au NPs. The Au content in studied Au NP infiltrated PE-coated sphere opals is 49 and 59 wt % for samples made of four and eight PE-coated spheres, respectively. The NPs mostly occupy the interstices of the opals, as demonstrated by scanning electron microscopy (SEM), and impregnated opals preserve a face centered cubic (fcc) symmetry of bead packing (Fig. 1). Altering the number of PE layers and the NP impregnation time allows tuning of the amount of gold. A shortcoming of this approach is the lack of control of the metal density depth profile in the opal, which prevents a precise correlation of the optical spectra to NP loading. In the following, we denote these opals as Au-infiltrated opals to distinguish them from Au-coated opals, which are assembled from Au nanoshells.
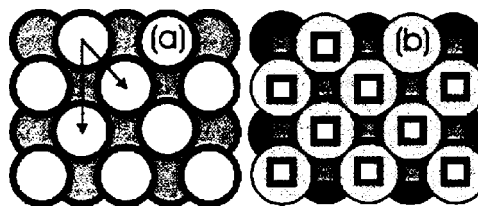

FIG. 1. Schematics of metal shells in Au-coated (a) and Au-infiltrated (b) opals. Circles (squares) represent Au-coated spheres (O shells). The darker the circle (square) the more distant it is from the figure plane. T shells connecting O shells are not shown for simplicity.

[a)]On leave from Ioffe Institute, St. Petersburg, Russia.
[b)]Author to whom correspondence should be addressed; electronic mail: sergei.romanov@nmrc.ie
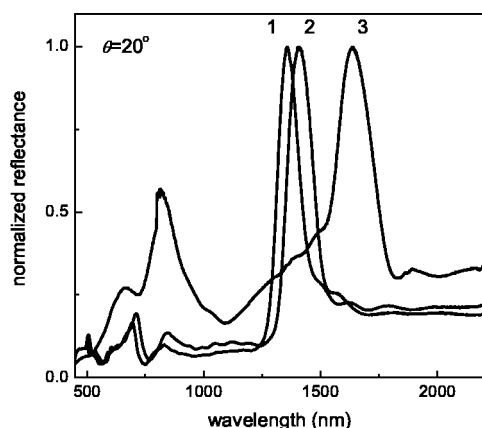
FIG. 2. Reflectance of bare opals (curve 1) and opals from the same beads coated with 8 PE layers before (2) and after infiltration with Au NPs (3).

FIG. 4. Reflectance of 59 wt % Au-infiltrated opals at different angles. Spectra are shifted vertically for clarity and labeled by angles of incidence. Arrows indicate SPR bands.

The samples were illuminated by a 1-mm-diam collimated beam of white light from a halogen tungsten lamp. Reflectance was measured in the mirror configuration at the same angle with respect to the [111] axis of the fcc lattice as the angle of light incidence, θ. An aperture was used to select the reflected light within 5° of the solid angle along the detection direction to obtain angle-resolved reflectance spectra.

The (111) diffraction resonance of opal of PE-coated PS beads is "red" shifted compared with that of the opal made of uncoated PS beads due to the lattice parameter increase (Fig. 2).[5] Both opal films have similar crystal quality, as assessed from the resolution and width of the resonance peaks in reflectance spectra. Further redshift of the (111) diffraction resonance after Au NP infiltration occurs due to the increase of the lattice parameter and changing the effective refractive index (RI) of the ensemble. Owing to complex contribution of NP dielectric constant, a precise evaluation of the diffraction resonance is out of the scope of this study.

The development of SPR bands of Au nanoshells follows the increase of Au NP loading. SEM data indicate only 6% increase of the bead diameter in the 49 wt % Au-infiltrated opal with respect to bare opal from 640 nm beads,[5] thus leaving the lattice parameter practically unchanged in the opals with spectra 1–3 of Fig. 3. Simultaneously, the number
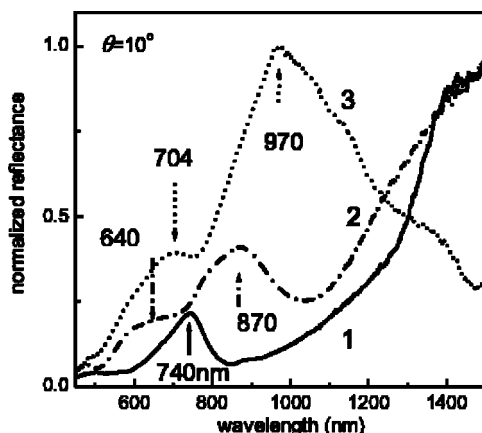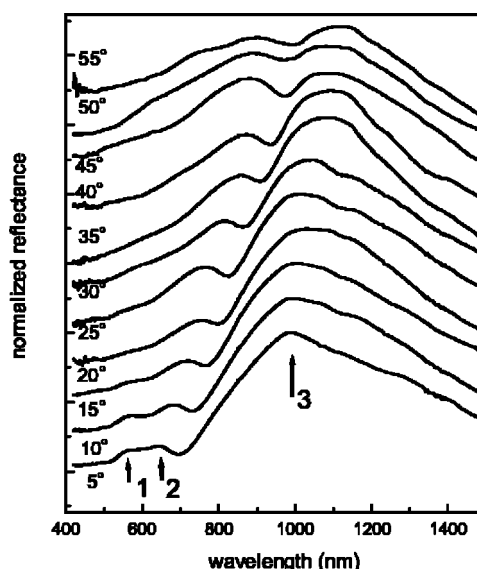

FIG. 3. Reflectance of Au-infiltrated opals with increasing Au NP loading. The number of PE layers increases from two to four to eight for spectra from 1 to 3, respectively. Arrows indicate SPR bands.

of PE layers increases by four times, yielding an essential increase in the Au NP coating thickness. The SPR reflectance band of lightly loaded opals is centered at ~740 nm. Following an Au loading increase, the SPR splits into two bands, moreover, both bands shift to longer wavelength. The long wavelength band increases its intensity and width at higher loading, hence in the highly loaded opal the short wavelength band appears as a satellite to the long wavelength band.

A well-known redshift of the SPR of Au NPs in a "heavy" dielectric environment and NP aggregation explains the enhanced reflectance in the range 550–620 nm.[8] In the case of stand-alone nanoshells, the SPR spectrum consists, mainly, of two dipole bands. The bandwidth of the long wavelength one, which relates to the nanoshell cavity and depends on cavity size and shell thickness,[9,10] can be very broad, extending to the NIR.[11] The latter is similar to the long wavelength SPR band in Fig. 3. The rule that the SPR wavelength decreases with increasing shell thickness for the same total nanoshell diameter applies to individual nanoshells.[12] The opposite trend of changing the SPR wavelength in Au-infiltrated opal points to the crucial role of interactions between nanoshells in the dense lattice. For example, the calculated reflectance of two-dimensional (2D) metal PhC predicts the dramatic spectrum variation depending on the metal filling fraction.[13] Additionally, a number of multipole resonances with interaction-dependent intensities fill the spectral range between dipole resonances.[14]

SPR bands in the reflectance spectrum of Au-infiltrated opals behave differently along the observation angle increase: the 570 nm band remains at the same position but quickly disappears, while the 645 and 985 nm bands shift to longer wavelengths and the intensity of 645 nm band increases progressively with respect to that of the 985 nm band (Fig. 4). In contrast to the Au-infiltrated opal, which shows one nondispersive and two dispersive bands, in Au-coated opals there is no shift for all but one band (Fig. 5). The
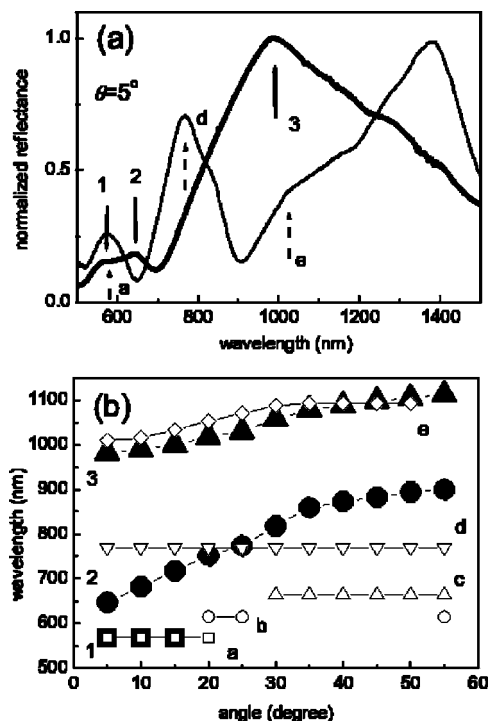
FIG. 5. (a) Reflectance spectra of 59 wt % Au NP-infiltrated (thick line) and 57 wt % Au-coated opals (thin line). SPR bands are indicated by numbers for the former and by letters for the latter. The 1370 nm band in Au-coated opal is the Bragg resonance. (b) SPR angle dispersion in Au-infiltrated (solid symbols) and Au-coated (open symbols) opals. Data for the latter are extracted from Ref. 6.

nondispersive "*a*" and "1" bands are the same in both types of opals and refer to dipole SPR of Au NPs. A similarity is also observed for "*e*" and "3" bands, which show a redshift with increasing angle [Fig. 5(b)]. These bands can be tentatively assigned to cavity dipole SPR. The SPR bands in the intermediate wavelength range, which are nondispersive in the Au-coated opal but dispersive in the Au-infiltrated opal, are, probably, those due to nanoshell interaction.

While two opal types are similar in terms of the Au loading and lattice constant, they differ with respect to the topology of the Au NP coating. In Au-infiltrated opals NPs occupy the PE layer on walls of octahedral (*O*) and tetrahedral (*T*) interstices,[15] since the NP diffusion is suppressed in areas where the beads are in contact with each other. In this case, the sample is an ensemble of air-core *T* and *O* nanoshells of $0.23D$ and $0.41D$ size, respectively, embedded in a polymer. In turn, Au-coated opals are assembled from spherical *D*-size nanoshells (Fig. 1). The spatial homogeneity of the filling fraction and shell uniformity in Au-coated opals result in well-resolved resonance bands, whereas the insufficient size difference between *O* and *T* nanoshells of Au-infiltrated opals and infiltrate disorder are likely factors contributing to merging the resonances in a broad 985 nm band [Fig. 5(a)]. We noted that fitting the diffraction resonance wavelength requires the average RI of 1.57 for the 59 wt % Au-infiltrated opal and 1.26 for the 57 wt % Au-coated opal, which is either more or less than the RI of 1.38 of the parent

PS opal. This difference is likely to be interpreted in terms of the sample morphology.

The angle-dependent changes in SPR reflectance spectra of Au opals are reasonable to discuss in terms of the nanoshell interaction. This approach can be justified by noting the connection between the ~30° interval of SPR intensity variation with respect to the internal angle θ_{int} of the light propagation and the 30° oscillation of the nearest neighbor distance in the Au-coated opal lattice [Fig. 1(a)] Similarly, in the Au-infiltrated opal the kink at $\theta_{int} \approx 30°$ is observed in both dispersive branches of the SPR. Thus, considering the directionality of the nanoshell density in a lattice one can expect the variation of the number and the intensity of lattice SPRs with respect to the direction of the incident beam. To what extent this approach can describe observed SPR remains to be addressed by modeling.

To summarize, reflectance spectra of Au-infiltrated opals based on 640 nm beads show unique behavior. The spectral separation of SPRs from the diffraction resonance allows considering them separately. The specific features of the SPR resonance in Au-infiltrated opals are both the effective redshift and changing the SPR reflectance intensity with increasing observation angle in contrast to mostly changing the SPR band intensity in lattices of spherical nanoshells.[6] Our observations point to the topology-dependent nanoshell interaction as the decisive factor for the SPR dispersion and intensity as well as the average RI in densely packed lattices.

[1] Z. Wang, C. T. Chan, W. Zhang, N. Ming, and P. Sheng, Phys. Rev. B **64** 113108 (2001)

[2] W. Y. Zhang, X. Y. Lei, Z. L. Wang, D. G. Zheng, W. Y. Tam, C. T. Chan, and P. Sheng, Phys. Rev. Lett. **84**, 2853 (2000).

[3] C. Graf and A. van Blaaderen, Langmuir **18**, 524 (2002).

[4] S. J. Oldenburg, S. L. Westcott, R. D. Averitt, and N. J. Halas, J. Chem. Phys. **111**, 4729 (1999).

[5] Z. Liang, A. S. Susha, and F. Caruso, Adv. Mater. (Weinheim, Ger.) **14**, 1160 (2002).

[6] P. T. Miclea, Z. Liang, A. S. Susha, F. Caruso, C. M. Sotomayor Torres, and S. G. Romanov, Appl. Phys. Lett. **84**, 3960 (2004).

[7] S. G. Romanov, C. M. Sotomayor Torres, A. Susha, Z. Liang, and F. Caruso, Proc. SPIE **5450**, 34, (2004); D. A. Mazurenko, A. Moroz, C. N. Graf, A. van Blaaderen, and J. I. Dijkhuis, *ibid.* **5450**, 569.

[8] M. Quinten, Appl. Phys. B: Lasers Opt. **73**, 317 (2001).

[9] E. Prodan and P. Norlander, J. Phys. Chem., **120**, 5444 (2004).

[10] S. Coyle, M. C. Netti, J. J. Baumberg, M. A. Ghanem, R. P. Birkin, P. N. Barlett, and D. M. Whittaker, Phys. Rev. Lett. **87**, 176801 (2001).

[11] S. L. Westcott, J. B. Jackson, C. Radloff, and N. J. Halas, Phys. Rev. B **66**, 155431 (2002).

[12] S. J. Oldenburg, R. D. Averitt, S. L. Westcott, and N. J. Halas, Chem. Phys. Lett. **288**, 243 (1998).

[13] T. Ochiai and K. Ohtaka, Phys. Rev. B **69**, 125106 (2004).

[14] J. E. Inglesfield, J. M. Pitrake, and R. Kemp, Phys. Rev. B **69**, 233103 (2004).

[15] V. G. Balakirev, V. N. Bogomolov, V. V. Zhuravlev, Y. A. Kumzerov, V. P. Petranovskii, S. G. Romanov, and L. A. Samoilovich. Crystallogr. Rep. **38**, 348 (1993).